

# 3D Printing Locally Activated Visual-Displays Embedded in 3D Objects via Electrically Conductive and Thermochromic Materials

Kongpyung (Justin) Moon  
Industrial Design  
KAIST  
Daejeon, Republic of Korea  
jkpmoon@kaist.ac.kr

Ryo Suzuki  
Computer Science  
University of Calgary  
Calgary, Canada  
ryo.suzuki@ucalgary.ca

Zofia Marciniak  
Industrial Design  
KAIST  
Daejeon, Republic of Korea  
zofia.marciniak@kaist.ac.kr

Andrea Bianchi  
Industrial Design  
School of Computing  
KAIST  
Daejeon, Republic of Korea  
andrea@kaist.ac.kr

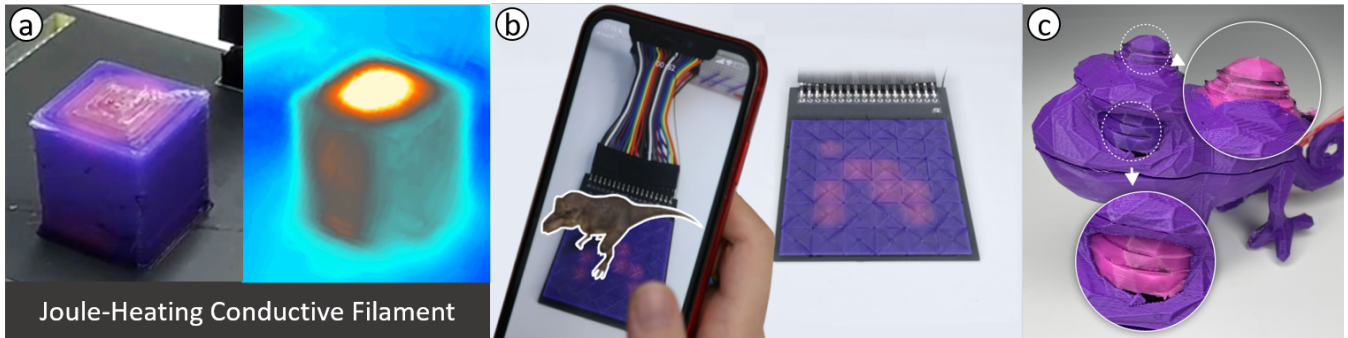


**Figure 1:** (a) A ThermoPixel can locally and selectively activate thermochromic material via Joule heating conductive filament. (b) Re-configuring AR marker on 6 × 6 matrix ThermoPixels. (c) 3D printed chameleon artifact that locally changes color on eyes and dorsal ridge

## ABSTRACT

3D printed displays promise to create unique visual interfaces for physical objects. However, current methods for creating 3D printed displays either require specialized post-fabrication processes (e.g., electroluminescence spray and silicon casting) or function as passive elements that simply react to environmental factors (e.g., body and air temperature). These passive displays offer limited control over when, where, and how the colors change. In this paper, we introduce ThermoPixels, a method for designing and 3D printing actively controlled and visually rich thermochromic displays that can be embedded in arbitrary geometries. We investigate the color-changing and thermal properties of thermochromic and conductive filaments. Based on these insights, we designed ThermoPixels and

an accompanying software tool that allows embedding ThermoPixels in arbitrary 3D geometries, creating displays of various shapes and sizes (flat, curved, or matrix displays) or displays that embed textures, multiple colors, or that are flexible.

## KEYWORDS

Thermochromic Filaments; Color-changing Interfaces; 3D Displays; Local Heating; Multi-material Printing

### ACM Reference Format:

Kongpyung (Justin) Moon, Zofia Marciniak, Ryo Suzuki, and Andrea Bianchi. 2024. 3D Printing Locally Activated Visual-Displays Embedded in 3D Objects via Electrically Conductive and Thermochromic Materials. In *Proceedings of the CHI Conference on Human Factors in Computing Systems (CHI '24)*, May 11–16, 2024, Honolulu, HI, USA. ACM, New York, NY, USA, 15 pages. <https://doi.org/10.1145/3613904.3642537>



This work is licensed under a Creative Commons  
Attribution-NonCommercial-NoDerivs International 4.0 License.

CHI '24, May 11–16, 2024, Honolulu, HI, USA  
© 2024 Copyright held by the owner/author(s).  
ACM ISBN 979-8-4007-0330-0/24/05  
<https://doi.org/10.1145/3613904.3642537>

## 1 INTRODUCTION

Desktop 3D printers facilitate the creation of complex physical 3D objects directly from digital models. Harnessing the innate properties of thermoplastic filaments, 3D printed objects can be augmented with functional properties such as capacitive sensing [11, 39, 40] and

mechanical actuation [2, 29, 42, 50, 51]. 3D printed visual displays crafted from thermochromic color-shifting filaments are another emerging type of functional 3D printed prototypes. Thermochromic materials, which alter their color in response to heat (around 32°C) and return to their original hue upon cooling, offer the potential to enhance functional 3D printing with objects that incorporate an integrated visual interface. Examples of such applications include a bracelet for body temperature sensing [5], and artifacts that change color when heated for handwork [23].

While these color-changing displays embed visual cues directly within the printed objects without requiring assembly of electronic components (e.g., Liquid-crystal display (LCD) modules and LEDs), and additional post-fabrication process [5, 23], they are, however, *passive* elements that merely respond to the environment (e.g., body heat or a heat gun), with limited control over the timing, the location, and the modalities in which the colors change. The simplicity of *passive* thermochromic materials comes with a trade-off in terms of limited functionality and versatility. Particularly, global heating diminishes the practicality of thermochromic filaments, as it depends on external equipment like hot air blowers and offers limited control, potentially risking damage to 3D printed objects through excessive heat. In contrast, thermochromic ink applied on paper or fabrics [9, 45] is a feasible option for constructing visually rich flat displays. These works by selectively and *actively* heating electrically conductive paths beneath the thermochromic ink, resulting in visual interfaces that are controllable and predictable on 2D substrates.

Inspired by these works, we propose a method for designing and printing visually rich but *active thermochromic displays* that can be embedded in arbitrary curved surfaces of 3D printed artifacts. Like prior work with paper or fabric, these displays rely on selective resistive heating via conductive filaments, resulting in color changes that are predictable, timely, and localized. This paper delves in detail about the formulation and design of a color-changing pixel primitive—the ThermoPixel—, which consists of a compound multi-material structure made of a thermochromic shell and an embedded resistive carbon-based heater. When current is supplied to the heater, the ThermoPixel structure heats up selectively and predictably, causing the surrounding shell to change color without damaging the geometry's neighboring part. This independent control allows for constructing complex displays of various shapes and sizes (flat, curved, flexible, matrix displays), which serve different purposes and enrich the design space for functional 3D printed prototypes. Moreover, our software interface allows users to select and embed ThermoPixels within 3D objects, focusing on the high-level functionalities and appearance of the visual displays. The seamless integration of visual displays into ordinary 3D printed objects holds significant potential for creating functional 3D printed artifacts. To summarize, we contribute:

- (1) The design, development, and evaluation of ThermoPixels, a primitive for a 3D printed color-changing interface that can be locally and selectively activated. This is complemented by evaluations of the properties of thermochromic and conductive filaments that form the rationale for conceptualizing ThermoPixels and assist users in incorporating ThermoPixels into their 3D printed prototypes.

- (2) An open-source software pipeline with a step-by-step walk-through that allows users to design and fabricate thermochromic displays on arbitrary curved surfaces.
- (3) The illustration of the design space for ThermoPixels with exemplary applications of 3D printed color-changing displays of different shapes, sizes, materials, colors, and functionality.

## 2 RELATED WORK

Our work is closely related to the literature on fabricating ink-based 2D and 3D displays and the use of thermochromic materials for visual interfaces.

### 2.1 2D ink-based displays

Fabricating custom-shaped *visual displays* (from now on, referred to these simply as *displays*) has been a subject of interest in recent HCI research. Electroluminescence (EL) ink, which emits light in response to the electrical current, has been widely applied to create custom displays on 2D surfaces. *Illumipaper* [22] and *PrintScreen* [32] introduced ink-injected 2D displays to render dynamic status information, like those in digital screens, but the display can be rolled and folded like physical paper. Similar to EL inks, Electrochromic (EC) ink, which changes color in response to the electrical current, can also be applied on 2D surfaces to fabricate custom-shaped displays. *TransPrint* [17] shows a non-light emissive color-changing interface on a transparent and flexible polymer sheet. Furthermore, *ECPlotter* [18] introduces a toolkit for rapidly prototyping EC displays through a custom-built machine that deposits conductive, dielectric, and EC ink in a predefined order. Electronic ink (E-ink) is another alternative and widely known material used for dynamic displays. Sweeney et al. [43] and Hanton et al. [13] introduce how E-ink can be printed and personally fabricated on various 2D shapes and objects by up-cycling existing devices (e.g. Amazon Kindle). While these ink-based displays allow the creation of a customized visual interface, they are either limited to 2D surfaces or require a manual but delicate fabrication process.

### 2.2 3D ink-based displays

Incorporating 3D displays into ordinary objects shows great potential for interactive and ubiquitous physical interfaces. However, accomplishing this is a challenging task, prompting a surge of recent research dedicated to the development of novel fabrication techniques. Su et al. [41] and Kong et al. [24] introduce 3D printed flexible organic light-emitting diode (OLED) displays, demonstrating a proof-of-concept fabrication pipeline for placing light-emitting diodes on curved surfaces. However, these technologies are confined to labs that have access to specialized printers that extrude metallic nanoparticles and nanoelectronic components [24, 41].

*ProtoSpray* [14], a recent work on 3D printed displays, uses Electroluminescence (EL) sprays on top of a 3D printed conductive object, eliminating the masking process typically necessary for fabricating EL displays. *ProtoSpray* can fabricate displays with individual pixel control, and on curved surfaces, such as a dome and wavelength geometries, enabling 3D printed artifacts to embed light-emitting displays, with varied choice of color inks. While this work has greatly advanced the fabrication process for 3D visual printed interfaces, it also inherits the limitation of spray-based

displays by adding post-printing fabrication steps that require time-consuming and hands-on skill such as uniformly applying paints in multiple layers (for dielectric and phosphor material), cleaning or changing the airbrush to prevent any ink contamination from other paints, and finally, demanding hours for drying the paint [26, 52].

Another fabrication method for producing a visual interface is using photochromic materials. *ColorMod* [36] 3D prints dense layers of photochromic ink, and *Photo-Chromeleon* [19] allows to re-color 3D printed objects over and over via coating with photochromic ink. However, both approaches require external devices such as a camera for calibration, and a UV light source or a projector to re-color the objects.

### 2.3 Thermochromic materials for displays

Thermochromic materials change color in response to heat, usually around 32°C, and revert when cooled. This reversible process has led to their use in flat, dynamic displays. For example, *Phosphenes* [45] employs thermochromic watercolor on a heating plate to create 2D interactive art. More recently, *Thermotion* [55] presented a 3D graphical interface animated via fluid channels. However, this requires a complex fabrication process involving 3D-printed molds, manual heating layers, and thermochromic inks, controlled by hydraulic circuits with hot water tanks [55]. While there are other efforts using thermochromic textiles [9], paper [25], and hydrogels [53], they are primarily limited to 2D displays [9, 45].

Pushing beyond flat surfaces, several recent works [5, 23, 55] have used thermochromic filament in 3D printed objects to create visual interfaces for various geometries. For instance, Djukanović et al. [5] presented a 3D printed wearable watch with thermochromic material to indicate the user's body temperature, which changes its color from grey to orange when the body temperature goes above 37°C (i.e., indicating fever). *ChromoFilament* [23] 3D prints thermochromic material as a visual temperature sensor that indicates when hot air is blown onto a printed object. Upon heat, the material color changes and indicates which part of the surface are malleable enough to be handworked.

While thermochromic material has already been introduced for 3D printed objects [5, 23], these examples are limited to passive visual sensors, which simply respond to environmental temperatures. In contrast, our paper motivations are closer to those of 2D thermochromic displays printed on paper [45] and textiles [9]. As in these works, we also use heat as a source of stimulus for selective activation of color-changing properties, but we expand this approach to 3D printed objects, diverging from the 2D focus of previous works. Although our work shares similarities with *Thermotion* [55] and *ProtoSpray* [14], our method sets itself apart by facilitating localized activation of thermochromic elements through carbon-based conductive filaments, and obviates the need for intricate, manual fabrication procedures.

## 3 THERMOPIXEL: A THERMOCHROMIC VISUAL MODULE

This section presents the design, development, and technical evaluation of a ThermoPixel—a self-contained primitive representing a single visual pixel for a 3D printed thermochromic display. It can be turned *ON* and *OFF* independently of other pixels, and its

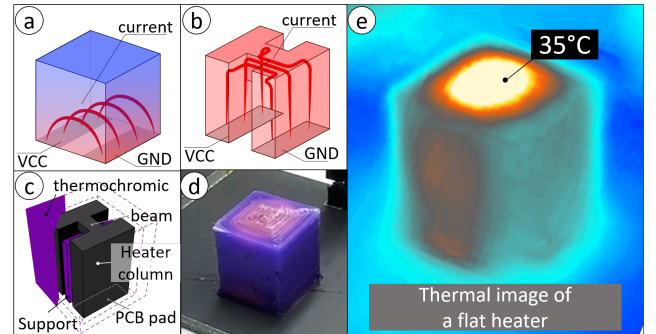


Figure 2: (a) Naive heating design approach in which current passes through the closest possible path (b) ThermoPixel heater structure in which current flows through the top surface of the geometry (c) ThermoPixel structure diagram (d) the image of color-changing ThermoPixel's top surface (e) Thermal image view of the ThermoPixels.

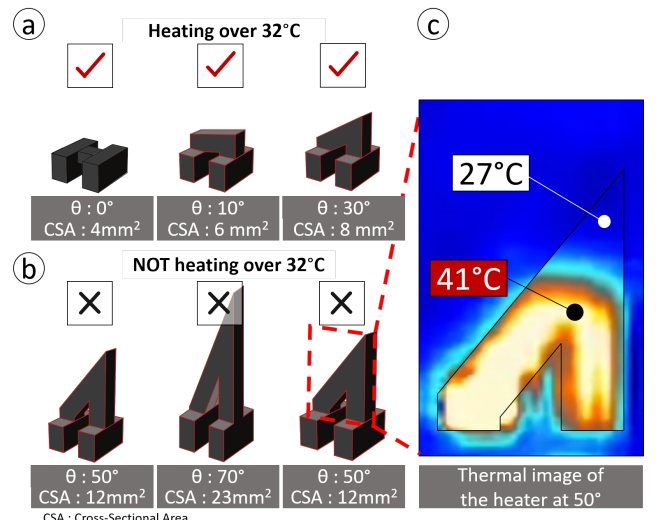
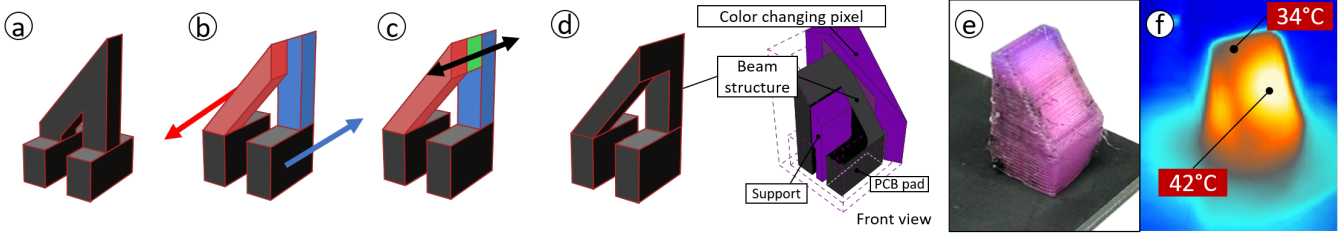


Figure 3: (a) heater design from flat to angle 50° (b) heater structure above angle 50°. (c) Thermal image of heater structure with an angle of 50°, in which heat is not fully distributed across the entire geometry.

activation results in a color-shift of the pixel's hue. Structurally, a ThermoPixel is a compound geometry consisting of two integral components: an *outer shell* made of thermochromic material and an *inner heater* made of conductive material (Figure 2c). Its design was guided by the material analyses outlined in section 6.

The thermochromic shell completely surrounds the inner heater and has a thickness between 1 and 8 mm. Only the upper surface of the shell serves as the color display, while the rest provides thermal insulation to the module, ensuring that heat remains as much as possible contained within the ThermoPixel and minimizing thermal dissipation to neighboring ones.



**Figure 4:** (a) Original slanted angled heater design (b) Slanted beams are moved to opposite sides (c), and a bridge is placed to connect the beams. (d) New heater design with equal cross-section across the beam. (e) image of activated ThermoPixels with slanted angle (f) thermal image of its heat distribution.

The internal heater is a conductive structure that approximates the surface normal of the outer shell. It is made of two vertical *columns* and a flat or slanted bridge connecting these. Each column has a footprint measuring 6x2 mm, a cross-sectional area of 12 mm<sup>2</sup>, and a variable height between 4 mm and 40 mm. The bridge connects the columns with a smaller cross-section (4 mm<sup>2</sup>). This structure effectively guides the electrical current from the bottom of one column to the bottom of the other, passing through the narrow bridge and causing this to heat up (Figure 2b). That is because, as shown in prior work [29], along a single path, the area with the smallest cross-section (i.e., largest resistance) is also the one with maximum power/heat dissipation (as explained by the equation  $P=I^2R$ ). This configuration ensures that the top of the ThermoPixel is the hottest part of the module (i.e., >32°C) and that it is, therefore, capable of triggering the thermochromic effect of the shell (Figure 2).

### 3.1 Design of slanted surfaces

Curved surfaces of 3D objects require ThermoPixels to be tilted to approximate, at best, the surface normal and provide the maximum surface contact for convection heating. This requirement implies that the ThermoPixel top surface may be slanted or curved, adapting to the contours of the surface at any angle to accommodate various inclinations. This adaptability in the angle of a slanted surface is essential to the design and is reflected in the construction of the heaters. Based on the specific inclination needed for the top surface, we have developed two distinct slanted heater designs to meet these requirements.

Heaters that are angled up to 50° are conceptually identical to the flat ones. Simply, the two beam structures have different heights and connect those with a triangular slanted geometry (see Figure 3) that is parallel to the thermochromic layer (also tilted). However, this approach fails to work correctly for angles greater than 50°. In fact, as Figure 3c shows, the electrical current attempts to follow the path of least resistance, staying at the bottom side of the corner formed with the taller beam. As a result, the bottom part of the ThermoPixel is heated at 41°C, but the top part is only at 27°C. This causes the pixel to only be partially heated—which is, in fact, the very same problem that motivated the design of the bridge structure (see section 6).

Therefore, for angles greater than 50°, we solved this issue with a new design. As shown in Figure 4, we constructed a slanted

and a vertical beam at different positions (red and blue in the Figure). We then placed a connecting bridge between the tips of the beams. As Figure 4e shows, this new design ensures uniform current flow across the whole length of the beams, resulting in the thermochromic surface being fully activated (Figure 4f) and with a color-transition temperature above 32°C.

### 3.2 Technical evaluation of ThermoPixels

To characterize and evaluate the behavior of Joule-heated ThermoPixels, we conducted four studies aiming to answer the following questions: 1) How long does it take for ThermoPixels with shells of varying thickness to turn on? 2) What is the range of acceptable heights for the heating structures? 3) What is the maximum inclination a ThermoPixel can be oriented? 4) How does ThermoPixel affect the neighboring non-color-changing areas?

**3.2.1 Evaluation method:** All ThermoPixels were printed on a custom PCB with exposed pads (6x2 mm - Hot Air Solder Leveling (HASL) surface finish - Figure 19a). The PCB was routed to expose each pair of pads to an external power supply (Rhode and Schwards NGA100), so to avoid manual wiring (as in [10]), and at the same time, ensuring a consistent and reliable electrical connection between the power supply and ThermoPixels (Figure 19). Vias (0.4 mm) placed on the pads contributed to further strengthening the adhesion of the conductive filament with the copper substrate of the PCB (Figure 19c).

We ensured that all samples had a target resistance of 100 Ω (average: 93, SD: 5.8) through the annealing process (detailed in section 6.2.2.) and wired them to a DC power supply. After powering the samples with 100 mA for 60 seconds, we observed changes in color using an HD and a thermal camera (FLIR One). The video footage was used to compute, via a Python script, the duration of the color-change transition. We judged a transition to be complete when we observed the relative luminance ( $\Delta Y$ , where  $Y = 0.2126 \times R + 0.7152 \times G + 0.0722 \times B$ ) of the pixel's top surface reaching a plateau — a state when thermochromic material fully changes its color.

We chose to represent how color changed over time using the relative luminance instead of the individual RGB channels because the relative luminance best describes the color perception with respect to the human eye's adaptation state, and because it is a single linear measure that can capture the contribution of all RGB components [46].

All experiments were repeated three times, and reported the average value. In total we have tested 39 samples, (4 thicknesses + 4 heights + 4 angles + 4 distances (in one sample))  $\times$  3 sampling.

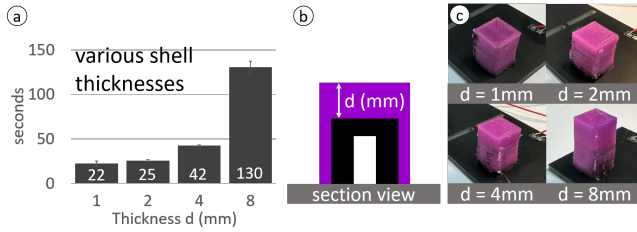


**Figure 5:** (a) Average color-change time of various shell thicknesses. (b) Diagram showing the thickness of the thermochromic substrate. (c) ThermoPixels with thermochromic top substrate printed in various thicknesses.

**3.2.2 Evaluation 1 – shell thickness:** To assess the time required for ThermoPixels with different thermochromic layer thicknesses, we 3D printed four samples with shell thickness values of 1mm, 2mm, 4mm, and 8mm. These samples were then Joule heated using a DC power supply, and we reported the average time to color-change in Figure 5a. The result shows that the thick layers of thermochromic material take longer to change color. We report a range between 22 (SD: 5) to 130 (SD: 11.3) seconds for the thinnest and the thickest samples, respectively, but we note that, with the exception of the 8 mm thick sample, all activations happen within 42 seconds. One possible reason that explains these findings is that, in our setup, thicker shells had a larger surface area exposed to the air convection (e.g., the sides of the sample), slowing down the heating process.

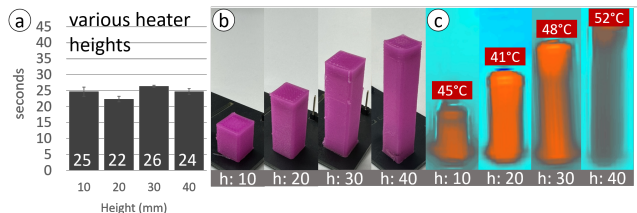


**Figure 6:** (a) Average color-change time of various heights of conductive heaters. (b) 3D printed ThermoPixels with varying heater heights all color changed. (c) Their thermal image view of various heater heights, the temperature values are measured from the top surfaces.

**3.2.3 Evaluation 2 – heater height:** For the second study, we printed ThermoPixels with the heater height of 10, 20, 30, and 40 mm tall with an equal thermochromic layer thickness of 1 mm. We reported the average time of color-change of various heights in Figure 6a. As a result, we report an average activation range of 24.5 s (SD:2, min:22 max:27). It is important to recognize that these outcomes would not be achievable with heaters that are merely

cuboid in shape (as we have experimented in section 6.2), as the current would flow only at the bottom of the heater in such a design (Figure 20).

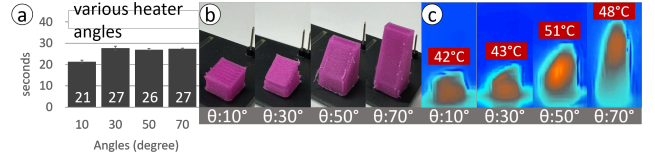


**Figure 7:** (a) Average time color-change time of various angles. (b) 3D printed ThermoPixels with varying angles all color changed. (c) Their thermal image view.

**3.2.4 Evaluation 3 – heater angle:** To assess the uniform heating of ThermoPixels across various angles, we 3D printed ThermoPixels at four different angles (10°, 30°, 50°, and 70°). For angles greater than 50°, we designed them with a slanted heater structure, as depicted in Figure 4. Figure 7a presents the average time it took for all four angles to change color when locally heated. Notably, all samples successfully achieved proper heating as the top surface temperature is greater than the color activation temperature ( $>32^{\circ}\text{C}$ ), as depicted in Figure 7c. The average activation time was 25.8 seconds (SD: 2.8, Minimum: 20, Maximum: 29) for all samples to fully color change (Figure 7b).

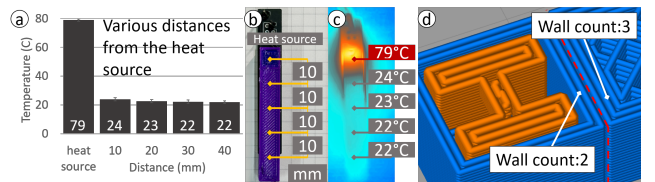


**Figure 8:** (a) Average temperature when heated for 60 seconds. (b) 3D printed sample image. (c) Thermal view of the sample. (d) Printing path visualization from the 3D printer's slicer.

**3.2.5 Evaluation 4 – surrounding area:** Lastly, to assess the impact of heat generated by a single ThermoPixel on nearby areas that do not change color, we created a 55 mm long test sample featuring one ThermoPixel as a heat source (Figure 8b). The temperatures were measured and recorded over time in non-color-changing regions located at distances of 10 mm, 20 mm, 30 mm, and 40 mm from the heater.

The findings (illustrated in Figure 8c) indicate that the heat emitted from a ThermoPixel does not significantly influence adjacent non-color changing areas, a result attributed to the low thermal conductivity of PLA material [28]. Further, the thermochromic shell of the ThermoPixel contributes to this effect due to its separate printing pattern, not being printed in a continuous path (as shown in Figure 8d). This segmented printing approach further reduces the cross-plane thermal conductivity of the PLA [8]. Consequently, even a temperature of  $79^{\circ}\text{C}$  (SD: 1.2) generated by the ThermoPixel has a minimal impact on nearby areas extending up to a distance of 40 mm ( $22^{\circ}\text{C}$ , SD:1.6).

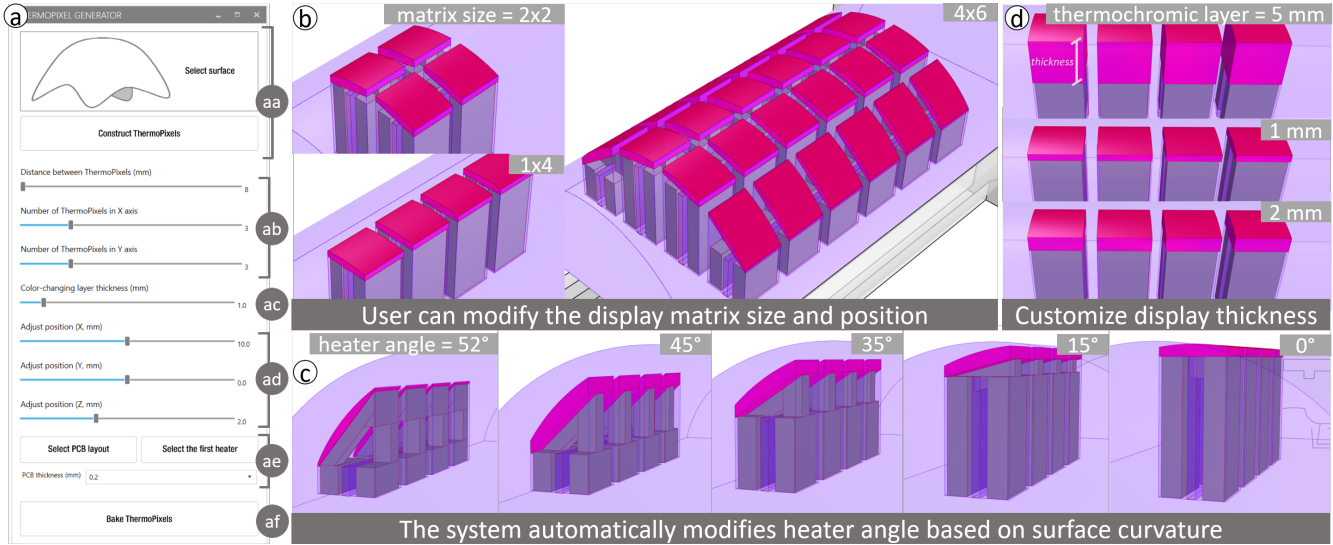


**Figure 9:** (a) A software user interface in Rhino environment. (b) ThermoPixels generated in various matrix sizes. (c) ThermoPixel's design modification based on curved surface. (d) Adjustable thickness value of thermochromic layer.

**3.2.6 In summary:** These four groups of technical evaluations demonstrate that the proposed ThermoPixel and heater design work correctly regardless of the pixel's height, inclination, and amount of thermochromic material placed on top of it. Additionally, the heat generated from a ThermoPixel does not significantly affect the surrounding neighboring non-color-changing areas due to its low thermal conductivity. For practical applications, we recommend using thermochromic shells in the range 1-4 mm, though shells up to 8 mm operate correctly (but require longer exposure to heat, so longer time). Based on these insights, we now focus on the design of displays composed by different arrangements of ThermoPixels, and we present a tool that allows designers to embed these structures in arbitrary curved surfaces.

#### 4 THERMOPixel DESIGN TOOL WALKTHROUGH AND IMPLEMENTATION

To help users create the visual displays in 3D printed objects, we developed an open-sourced<sup>1</sup> parametric plugin for the Rhino 3D modeling tool utilizing Grasshopper<sup>2</sup>. The plugin is operated using a custom interface (Figure 9) and its main purpose is to automatically generate and place ThermoPixels heaters underneath the thermochromic surface of a 3D model. The model itself can be printed with multiple filaments, but the part of the geometry that constitutes the display must be printed with thermochromic filament, like the charge level indicators in the hand crank (Figure 10j). The local heaters, which are placed underneath, are printed with conductive materials, such as *ProtoPasta* [34].

The software interface (Figure 9a) consists of six features designed to aid users in integrating ThermoPixels into 3D geometries. Those features are (a) Choosing a target surface and embedding

ThermoPixels into the designated geometry; (b) Adjusting the size of the ThermoPixels matrix, including the number of pixels, and the distance between them; (c) Modifying thickness of the thermochromic layer; (d) Modifying the placement of the ThermoPixels grid along the X, Y, and Z axes; (e) Aligning PCB drawings with the ThermoPixel grid; (f) Integrating the designs into the Rhino platform for 3D printing purposes. Based on these user inputs, the software automatically generates and positions ThermoPixels within the chosen geometry.

#### 4.1 Walkthrough

To provide a comprehensive picture of the applicability and fabrication process of ThermoPixels, we demonstrate integrating four ThermoPixels on a 3D printed hand crank charger<sup>3</sup> to visualize charge level. The walkthrough is described in the following ten steps.

**Step 1:** Users import or draw a 3D geometry that they want to integrate color-changing displays and assign a target surface to the software by clicking the "select surface" button (Figure 10a). Once a target surface is assigned, the software, by default, generates a 3 x 3 matrix of ThermoPixels. The user can adjust the matrix size from 1 x 1 to a size that fits inside the target surface area (in our case, the maximum matrix size is 4 x 6, Figure 9b). Here, we set the size of the matrix to 1 x 4 to have a linear four-stage charging level (Figure 10b).

**Step 2:** Users can modify the ThermoPixels' position using the X and Y position sliders (Figure 9(ad)), and the ThermoPixels' heater structures update their angles corresponding to the curvature of the surface (Figure 9c). When the ThermoPixels are positioned outside

<sup>1</sup><https://github.com/makelab-kaist/ThermoPixels>

<sup>2</sup><https://www.grasshopper3d.com>

<sup>3</sup><https://www.thingiverse.com/thing:3767724>

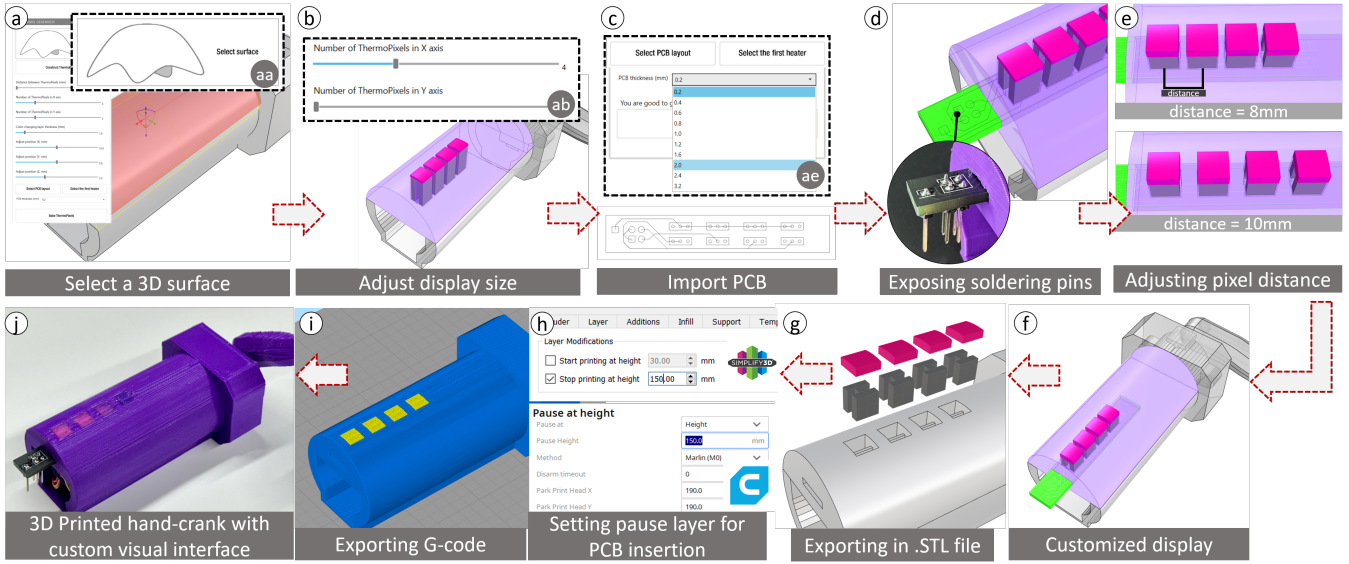


**Figure 10:** (a) Selecting a target surface to embed ThermoPixels. (b) Defining the size of the ThermoPixel matrix. (c) Importing PCB drawing in SVG file to align on to the ThermoPixels. (d) Adjusting position of the ThermoPixels to expose PCB's connector pins for soldering. (e) Adjusting distance between each ThermoPixels. (f) Fully generated ThermoPixel displays. (g) Exported to Rhino environment for 3D printing. Each components are saved in separate layers. (h) Users can set a pause layer during 3D printing to inser the PCB into the 3D printed model. (i) Generate G-code. (j) Final printed hand crank generator.

the target surface area, the interface warns the users to modify the settings.

**Step 3:** The thickness of thermochromic material is set to 1 mm as a default, as determined by our study (see section 6.1); users can customize thickness from 1 mm to 8 mm thickness (Figure 9d).

**Step 4:** Users can import a PCB drawing into the Rhino via Scalable Vector Graphics (SVG) file format, and can assign it to the software by clicking the 'select PCB' button, specifying its thickness value (Figure 10c).

**Step 5:** The software aligns the PCB's copper pads to the heater footprint of ThermoPixels (Figure 10d). It then updates the position of the PCB along with the ThermoPixels

**Step 6:** Once the first heater is aligned to the PCB, users can adjust the distance between the heaters. Since the PCB's copper pads are drawn with 10 mm spacing, we set our heater spacing to 10 mm (Figure 10e).

**Step 7:** The ThermoPixels' positions are adjusted on the X axis to expose the PCB's pin header connections for soldering (Figure 10d), and in the Z axis to reduce the resistance of the header geometry (see section 6.2).

**Step 8:** The software generates a void in the hand crank geometry tailored to the PCB's size, position, and thickness that allows the insertion of the PCB during the 3D printing process (Figure 10g).

**Step 9:** When users are satisfied with the design, they can bake the geometries into the Rhino environment in three separate layers: conductive heaters, color-changing displays, and non-color-changing objects that are prepared for 3D printing.

**Step 10:** Users can export the geometries to a 3D print slicing software, where they can set a pause command to insert the PCB during the 3D printing process. For instance, *Ultimaker Cura*, an open-sourced slicing software, allows users to pause at a specific height (in our case, 150 mm). *Simplify3D*, another widely used slicing software, can pause 3D printing at desired height through the "stop at height" feature (Figure 10h). After 3D printing (Figure 10j), users can solder male pin headers to the PCB's pin connectors (Figure 10d) for supplying electric current.

Our software interface allows a seamless way for users to incorporate ThermoPixels into their 3D designs. It continuously calculates and updates the angle of the heater, providing users with the flexibility to fine-tune ThermoPixels through adjustable parameters for desired integration.

## 4.2 Implementation

We developed software within Rhino Grasshopper using C# that seamlessly generates ThermoPixels while ensuring they conform to the curvature of the target surface. The implementation process starts by converting the input surface into a mesh structure, with each face having a maximum angle of 5° and edges limited to 10 mm. This conversion ensures adequate face numbers for forming any curved surface and prevents an excessive number of faces that may slow down the software. The ThermoPixel footprint, measuring 6 × 6 mm, is projected towards the Z axis onto the user-defined surface (Figure 11a). Utilizing the 'Evaluate Surface' component in Grasshopper, the interface calculates the normal vectors of each face within the ThermoPixel's projected area (see Figure 11a). We then calculate the average of these normal vectors for each region,

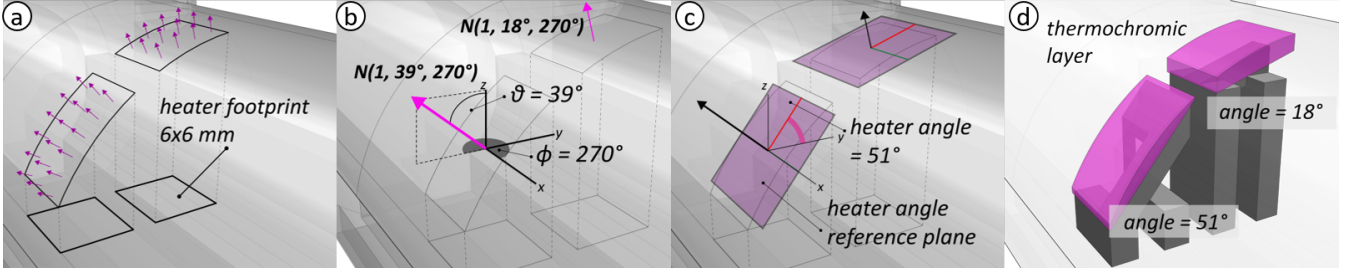


**Figure 11:** (a) The normal vectors of surfaces where ThermoPixels are located. (b) Getting the averaged normal vector for each ThermoPixels. (c) Generating the angled plane for heater generation. (d) Creating heater based on planes angle to the world XY axis with the thermochromic layer on top for color change.

as depicted in Figure 11b, and create a plane perpendicular to this average normal vector — which is  $N(1, 39^\circ, 270^\circ)$  as shown in Figure 11c. This reference plane aligns with the surface's curvature, and by calculating its angle in relation to the world axis, the software determines the specific type of heater structure ThermoPixel needs. For example, in Figure 11c, the local plane is slanted at  $51^\circ$  to the world axis, prompting the software to create a corresponding slanted heater (Figure 11d), as detailed in Figure 4. Lastly, the interface establishes a thermochromic display layer, defaulting to a 1 mm thickness, which is adjustable by moving the reference plane along the Z axis (Figure 11c).

## 5 DESIGN SPACE OF THERMOPIXELS WITH EXEMPLARY APPLICATIONS

This section showcases four types of color-changing displays that can be embedded in 3D objects. Our design space includes displays that are 1) flat, 2) colored, embedded, and textured, 3) curved with arbitrary shapes, and 4) flexible. These layout configurations are achieved by combining individual ThermoPixels, each maintaining independent control from the others. Routing for these applications is done either using manual wiring or printing directly onto a PCB (Figure 13a).

### 5.1 Flat Displays

Flat displays, similar to traditional pixel screens, are well-suited for presenting information using text characters, pixelated images, seven-segment numerical digits, and more. These displays can serve as complementary tools to provide more detailed visual information, such as a day-of-the-week application (see Figure 14a) integrated into a desk photo holder accessory, or be combined to form a larger display (Figure 12).

In Figure 12, we present example displays suitable for integration into various applications. In Figure 12a-d, a  $6 \times 6$  square matrix display of 36 ThermoPixels is used as a medium for displaying a pixelated image of a smiley face (Figure 12b) and letter (Figure 12c). Furthermore, we employ a matrix display to visualize an AR marker (Figure 12a,d), which can be viewed using a decoding application (e.g., Adobe Aero) on a phone. Figure 12d-e showcases non-matrix examples of a flat display: a two-digit seven-segment display constructed using 14 ThermoPixels manually wired to the

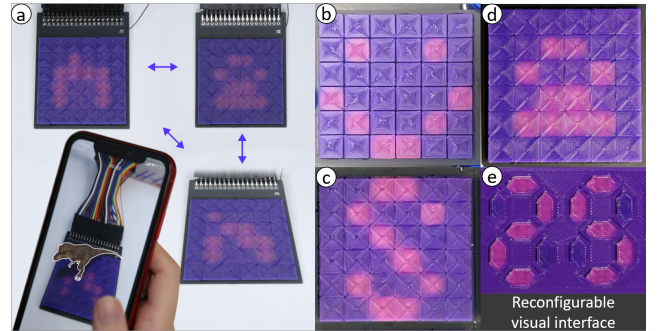


**Figure 12:** A Flat  $6 \times 6$  matrix display rendering (a) three augmented reality code from a single display, (b) smiley face emoticon, (c) letter "S", (d) AR code, and (e) two seven-segment display combined to render two digit number 25.

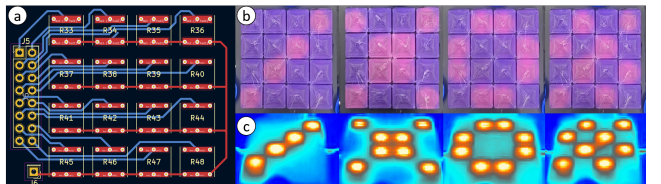


**Figure 13:** (a) Two-layered PCB design in Kicad. (b)  $4 \times 4$  matrix display with rendering diagonal (c) cross, (d) circle, and (e) checkerboard patterns from the same display.

power supply. For these displays, individual pixels are independently controlled, as seen in Figure 13. To achieve a compact form factor (pixels with a footprint of  $8 \times 8$  mm and 4 mm height) and simple routing to power, we printed the matrix directly on top of PCB substrates.

**5.1.1 Individual control through time-multiplexing:** It is also possible to control the display via time-sharing multiplexed PWM (Pulse-Width Modulated) signals (30V and 100mA) using a Maxim 3016 CPI [27] multiplexer chip (1 ms per each pixel). With this configuration, we were able to simultaneously and independently activate up to 8 pixels (Figure 13b- checkerboard) within 17.5 s (SD

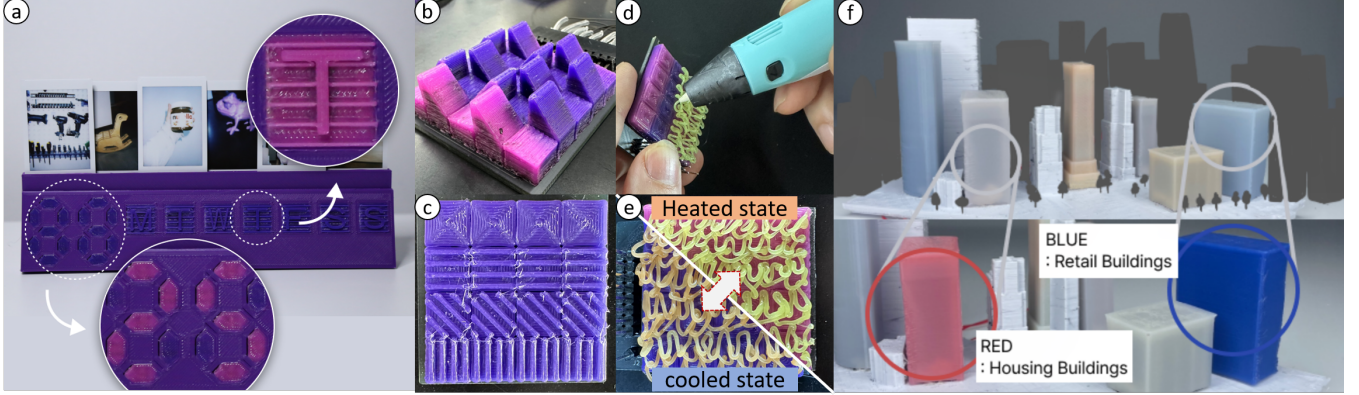


**Figure 14:** (a) A calendar photo-holder that selectively displays a day of the month from two-digit seven segment displays and a day of the week through a textured display.  $4 \times 4$  matrix displays with (b) differently angled tectonic surfaces, (c) small textural patterns for various tactility, (d) a hand-crafting texture with a 3D-printing pen, and (e) color-changed hand-crafted texture. (f) Infographic urban map with buildings color-changing to red, blue, and light orange individually when ThermoPixel is deactivated to represent building program.

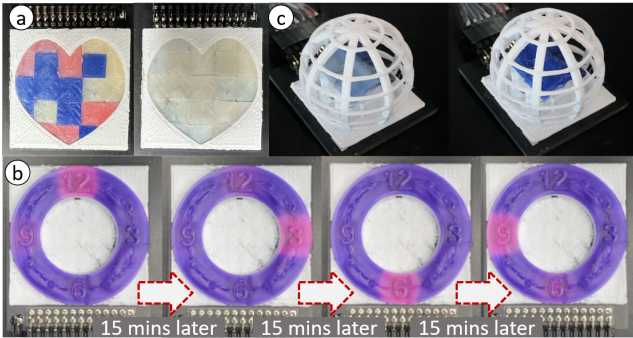


**Figure 15:** (a) A heart shaped display with multiple color (blue, red, and yellow) changes to white when activated. (b) A ring-shaped non-pixelated hour clock that sequentially and selectively activates every 15 minutes. (c) A color-changing roof embedded inside a sphere frame structure

= 1.1). We demonstrate a usage of this technique with a  $4 \times 4$  square matrix and a multiplexer in Figure 13. To quantify the time duration of color-change for pixels activated with time-multiplexing, we measured two extreme cases — when only one pixel and when all 16 pixels are ON — and reported the color-changing and cooling time. This process was repeated three times with identical samples. On average, one pixel took 7.3 seconds ( $SD = 1.1s$ ) to color-change and 478.7 seconds ( $SD = 3.5s$ ) to cool down to room temperature ( $25^\circ\text{C}$ ). On the other hand, the entire pixel matrix took 16.6 seconds ( $SD = 1.5s$ ) to color-change and 298.7 seconds ( $SD = 32s$ ) to return to the original color. These results show that cooling takes longer than heating ( $t_{ON} < t_{OFF}$ ), as also reported in previous work [23]. However, differently from previous *passive* thermochromic displays [5, 23] ThermoPixels can independently control each pixel and enables to re-purpose a display to deliver various information,

including emotions, characters, and digital data (i.e., through AR markers).

## 5.2 Textured, Embedded and Multi-Color Displays

Colors and textures are two ways to further enrich the visual look of the displays. Multiple colors can be achieved using thermochromic filaments with different pigmentation, while textures can be achieved by altering the surface of a 3D object or introducing geometric features. For the multi-color example, we presented a scaled city (see Figure 14f) where colors are used to represent different types of buildings. For this example, 24 ThermoPixels were embedded in the buildings of the scaled city. The buildings were made using white PLA, and blue, red, and orange thermochromic filaments [1]. Also, in Figure 15, a shows a pixelated heart display with three different colors (pink, blue, and yellow) turning into white when all pixels are activated.

Textured displays are flat displays that embed tactile properties. They are motivated by prior work [15, 21, 44], which attempted to bring tactile affordances to traditional flat screens. In the application in Figure 14a, textures were used to highlight the initials of the day of the week. Figure 14b-e shows more examples of texture displays with non-continuous, triangle-based tectonic surfaces integrated into a matrix display. To implement this, we used ThermoPixels slanted 10° or 60°. Figure 14c shows smaller texture patterns ( $1mm \times 8mm$ ) repeated in various directions, which did not require using slanted heaters. Figure 15b displays a circular clock interface constructed with 4 ThermoPixels, which indicate quarter-hour increments by activating a specific heater every 15 minutes. Textural patterns can also be hand-crafted directly on top of exposed heaters using thermochromic filament and a 3D pen (Figure 14d-e). Through this handwork, a user can achieve an intricate appearance or smooth rounded textures. Finally, the slanted blue roof within the geodesic dome transitions to white color upon activation of the

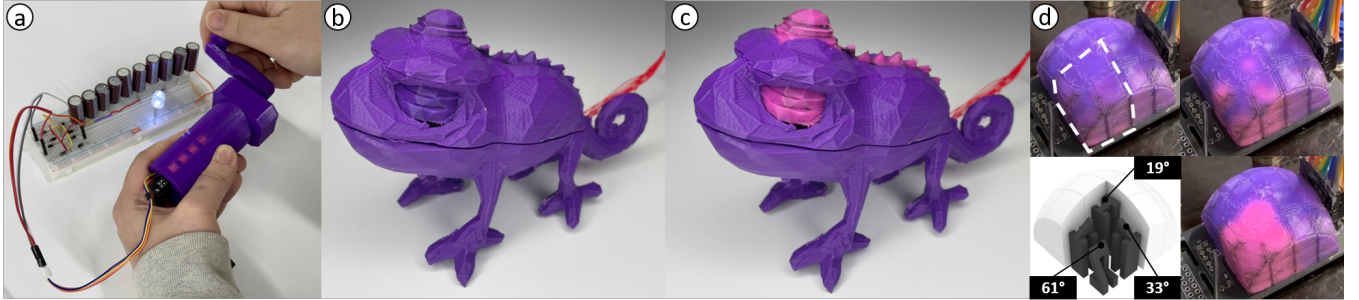


**Figure 16:** (a) A hand crank generator that has four ThermoPixels indicating charge level, and an LED that is turned on through the hand crank. (b-d) D printed chameleon changes the color of the eyes and dorsal ridge from purple to pink, when the ThermoPixels are activated. (d) A dome structure with angled ThermoPixels, that change its color simultaneously.

slanted ThermoPixels, demonstrating the feasibility of embedding a display within an object, made possible by the fully 3D printed nature of ThermoPixels.

### 5.3 Arbitrary Curved Displays

The main feature of ThermoPixels is that they can be embedded in arbitrary 3D objects. In fact, the ThermoPixels can be constructed and oriented to approximate any surface—granted enough volume for placing a ThermoPixel within a geometry (see next section for the implementation details). For example, Figure 16d shows a dome structure [14] constructed using 16 individual ThermoPixels, each uniquely slanted to approximate the dome surface, and arranged as a  $4 \times 4$  matrix. The matrix layout allows for partial activation of the dome (e.g., only a corner). Figure 16b-c show the 3D printed chameleon<sup>4</sup> with color-changing eyes and dorsal ridge. These turn pink when activated. Inside the chameleons, we placed nine ThermoPixels. Each eye requires two  $70^\circ$  angled heaters, and the dorsal ridge uses three  $60^\circ$  and four  $20^\circ$  angled heaters. Unlike the previous display where the ThermoPixels are allocated near to each other ( $\leq 10$  mm), heaters inside the chameleons are positioned distant from each other ( $\geq 50$  mm). Therefore, instead of using multiple PCBs, we manually wired the heaters to the power supply with silver paste (ELCOAT,  $1-3 \times 10^{-5} \Omega/\text{cm}$ ).

Finally, Figure 16a shows a 3D printed hand crank generator. The hand crank generates a DC to turn on the LED. We used a BYJ48 stepper motor connected to two rectifiers and ten 6.8V capacitors connected in parallel. ThermoPixels are embedded inside the cylindrical body of the prototype, indicating the charge level in 4 increments. For this application, we printed  $1 \times 4$  ThermoPixel matrix on a PCB (Figure 10d) and manually powered the heaters from an external power supply.

### 5.4 Flexible Displays

Thermochromic TPU filament [38] is a soft color-changing filament that provides an opportunity for 3D printing soft displays. Its material properties are well suited for printing flexible artifacts [5], but also meta-material structures [7, 16] with functional properties. For example, Figure 17 shows a  $4 \times 4$  cell structure that is activated either by row or by column depending on the shear direction of

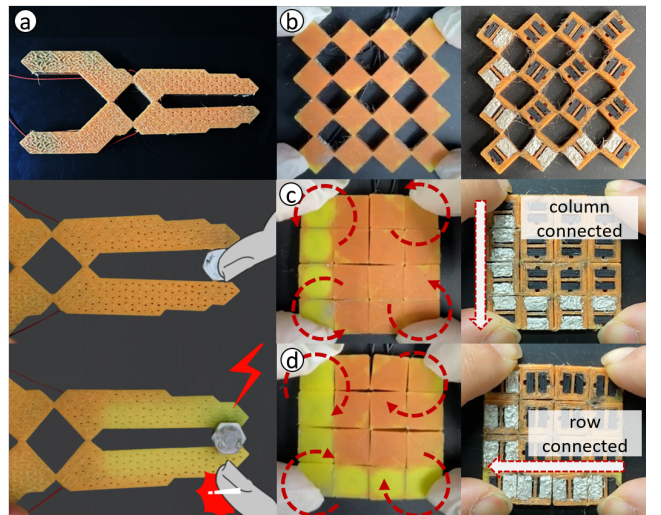


**Figure 17:** (a) A current sensing pliers that does not change any color when pinched a plastic bolt has no current flow, but changes its color from orange to yellow when it grips a metal bolt where current flows to the ground. (b)  $4 \times 4$  pixels meta-material structure printed using flexible thermochromic material with conductive heaters embedded in each cell. (c) Counter-clockwise rotation activates a column, while (d) clockwise rotation activates a row.

the cells. To enable the current to flow across cells we coated their inner walls with silver paste following previous work [7], although other methods that do not require post-processing are possible [48].

Another example is the pliers we previously introduced. These pliers are an example of a functional mechanical part, augmented by a thermochromic display placed at the tip that activates when a current is detected. These pliers were achieved by printing thermochromic flexible filament [38] for the plier structure and conductive filament [34] for the fourteen heaters, seven on each side of a plier.

<sup>4</sup><https://www.thingiverse.com/thing:1954181>

## 6 TECHNICAL EVALUATION OF THE MATERIALS: THERMOCHROMIC AND CONDUCTIVE FILAMENTS

To provide a base understanding for users to further customize and integrate ThermoPixels into their 3D printed prototype, we explore the properties of the two materials (thermochromic filament—*CC3D*: 24 USD / kg [3], and conductive filament—*ProtoPasta* [34]: 250–350 ohm/cm, 100 USD / Kg [34]) with two distinct technical studies. The primary objectives of these studies are: to gather numerical evidence that will inform the design of a *ThermoPixel*—a color-changing primitive structure that can be independently activated via resistive heating and that can form a display when combined with others (section 3). The questions we aim to answer in this section are the following: 1) How does the thickness of a geometry printed with thermochromic filament affect the overall color, and how long does it take for the color to change? 2) How is the temperature generated via resistive-heating distributed across the conductors?

### 6.1 Color Changes and Material Thickness

We designed an experiment to understand how long it takes for a sample cuboid printed with thermochromic filament to change color, and what is the cuboid optimal size. Since the specific heat capacity of a body is inversely proportional to its mass [47], we expected to see that larger cuboids have less vibrant color changes and take an overall longer time to activate.

**6.1.1 Material and method.** Using an FDM direct-drive printer (E3D Tool Changer), we printed four cuboids with different masses. We kept constant the footprint ( $10 \times 10$  mm) but varied their height (0.5 mm, 1 mm, 2 mm, and 4 mm). The layer thickness was set to 0.2 mm. We uniformly heated all the cuboids together at  $40^\circ\text{C}$  for a maximum duration of 180 seconds through the printer's heat bed. While doing so, we recorded an HD video of the cuboids for subsequent analysis of the color transitions and their timestamped heatmaps using a thermal infrared camera. We then measured the color intensity of the cuboids' top surface (facing the camera) until the temperature reached the nominal transition point of  $32^\circ\text{C}$ . All four samples were tested three times, with the heat bed being brought down to room temperature ( $24^\circ\text{C}$ ) before each trial. Overall, the study involved heating and measuring 12 separate samples.

To measure how long it took for the color-changing transition and what was the final color intensity, we wrote a custom Python script that computes the average variation of relative luminance from the pixels of the video frame, for all the frames and for each of the cuboids.

**6.1.2 Results.** Figure 18 shows the delta relative luminance ( $\Delta Y$ ) values over time for each sample size. All sample's colors shifted from their neutral color (i.e., purple) to the activated state (i.e., pink) once they reached the  $32^\circ\text{C}$  threshold. On average, this transition happened in 117 seconds ( $SD = 38$  seconds), with the thinnest sample taking the least amount of time (82 s,  $SD = 13$ ) and the thickest taking about twice the time (172 s,  $SD = 9.8$ ).

The first takeaway is that the thinner the thermochromic layer, the faster the activation is. However, we also note that the relative luminance of the smallest sample is about 3.5 times that of the

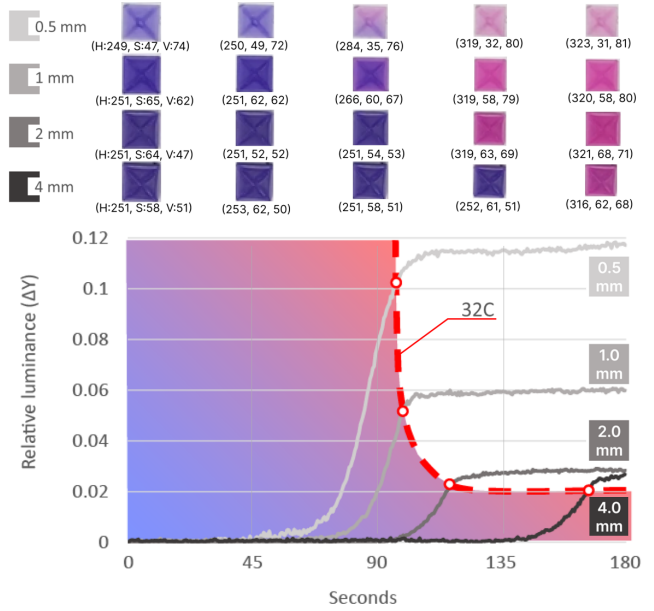


**Figure 18:** Four  $10 \times 10$  mm cuboid samples with various thicknesses are globally heated, and relative luminance over time is plotted.

thickest sample, probably due to the material's transparency when the color changes. In practice and based on our empirical trials, we recommend not to use thickness lower than 1 mm. Secondly, as expected, the luminance plateaued after reaching the threshold, despite how long a sample was heated. This implies that the heating does not have to be precise, but just sufficient to reach the activation point. Furthermore, the higher the heat (i.e., the thinner the sample), the faster the transition will be. For example, if we heated the printer's bed to  $80^\circ\text{C}$ , it would take only 31.2 seconds ( $SD = 0.9$  s) for the 1 mm sample to activate instead of 82 s (about 2.5 times faster).

### 6.2 Thermal Behavior of Conductive Filaments

Prior works demonstrated different methods to construct 3D resistive paths either through manual fabrication processes [12, 37] or by directly 3D printing an electrically conductive material [29, 49]. When a fixed current is then applied to the endpoints of this path, heat is dissipated proportionally to the path resistance—an effect known as resistive heating or Joule-heating [4]. Previous work reveals the relationship between the cross-section area of a geometry and the heat it generates [29], but the distribution of heat within the body of a geometry remains unknown. This study aims to empirically clarify this point.

**6.2.1 Material and method.** We printed four conductive cuboids ( $6 \times 6$  mm) with height ranging from 10 to 40 mm, in 10 mm intervals (Figure 20a) on a PCB (Figure 19) as in previous study (section 3.2.3). On the top of each cuboid we printed a 1 mm layer of thermochromic material that serves as a visual indicator of when the temperature reaches  $32^\circ\text{C}$ . The experiment consisted of applying a

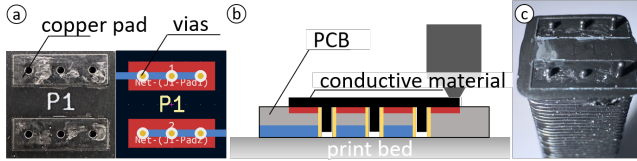


**Figure 19:** (a) PCB conductive copper pad with vias to create stable contact between the copper pad and conductive material. (b) Printing conductive material on top of PCB pads. (c) The base surface view of the conductive sample printed on top of a copper pad.

constant direct current at the base of the cuboid, while measuring how long it took for the color-changing layer to activate. As in the previous study, we both collected HD video footage and the heatmaps of the heated cuboids for offline analysis.

Before proceeding with the experiment and ensuring a fair comparison across samples, we had to account for differences in resistance among the cuboids, due to their size, printing imperfections, and the bondage between layers. For example, a quick inspection of our samples revealed that the resistance of the cuboids varied as much as  $40 \Omega$ , with the shortest samples (10 mm) measuring  $161 \Omega$  ( $SD = 13 \Omega$ ) and the tallest samples (40 mm) measuring  $121 \Omega$  ( $SD = 12 \Omega$ ). The problem is that, given a fixed current source, different resistances would cause unequal power consumption, following the equation  $P=I^2R$ , and so different heat dissipation. Thus, to avoid introducing a confounding variable we *equalized* the resistance of all the samples to a value that is lower than the closest rounded minimum ( $121 \Omega$ ) through the annealing method [6, 29].

**6.2.2 Equalization process.** This process is a short one-time Joule-heating process that reduces the resistance of the 3D printed geometry when the produced temperature exceeds the glass transition temperature of the material ( $70^\circ\text{C}$  [34]), creating stronger bondage between layers, thus forming a greater conductivity. This process was fully automated using a Python script for our programmable power supply. This method starts with measuring the initial resistance value, which sets a target resistance to stop at  $100 \Omega$ . The polymer-annealing equalizing process stops automatically, by controlling, via a Python script, the power supply when the resistance reaches the target value. To implement this, we built a simple circuit with an Arduino Nano and four relay switches (1 Channel 5V relay) that shut the current switch connected to the power supply when it reaches the target resistance and open another switch to equalize the next sample. After setting up the target resistance value, each sample is equalized to the target resistance by Joule-heating with 100 mA. Figure 20b shows the result of the resistance of all four samples after the equalization process. As a result, the average resistance of all samples is  $94 \Omega$  ( $SD = 4.5 \Omega$ ), regardless of their height. After the equalization process, the samples were Joule heated at 100 mA for 180 seconds to observe how heat was distributed across the cross-sectional area of the electrically conductive geometry. This experiment was conducted three times, and the average time it took for the thermochromic layer at the top of the samples to change color was reported.

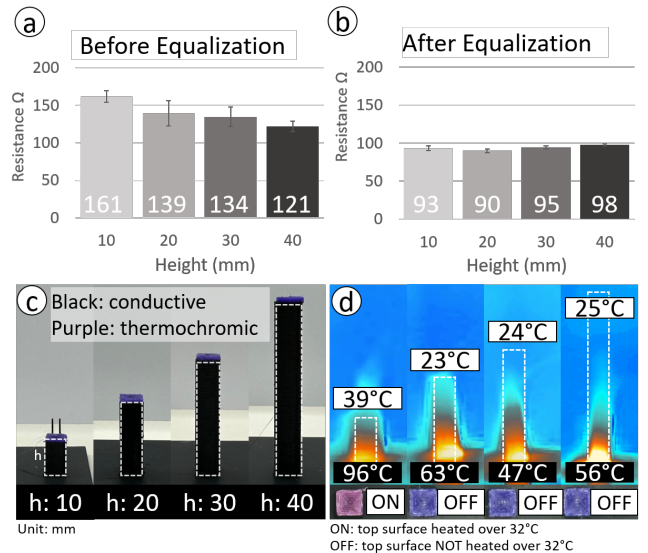


**Figure 20:** (a) Resistance of four conductive heaters before equalization, and (b) after equalization. (c) 3D printed four conductive heaters at different heights (10, 20, 30, 40 mm), and thermochromic material (1mm thickness) is printed on top of each heater. (d) Thermal camera view of the four samples

**6.2.3 Results.** Figure 20b shows that only the shortest among the samples was capable of activating the color-changing top thermochromic layer ( $39^\circ\text{C}$ ), with an average duration of 93.5 seconds ( $SD = 1.5 \text{ s}$ ). For the other samples instead, the temperature on the top layer never reached the color-transition threshold ( $< 32^\circ\text{C}$ ), leaving the color in its neutral state. On average, the temperature of these failed cases was  $8^\circ\text{C}$  ( $SD = 1^\circ\text{C}$ ), cooler than the activation temperature. However, more interestingly, the temperature at the base of all cuboids was never below  $47^\circ\text{C}$ .

The issue with cuboids of different heights is not that they are unable to produce enough heat for the thermochromic reaction to happen, but rather the fact that the heat is concentrated at their base instead of the top—in the proximity of the contacts with the pads. The reason for this is that the current follows the path of least resistance, which is along the horizontal printing path and never across the layers in the z-axis (as the adhesion between layers always results in higher resistance). We conclude that the naive design of heaters with simple cuboids does not work, but that instead, a proper design should consist of a path that *forces* the current to flow through the body of the cuboid across the z-axis, reaching its top surface.

### 6.3 Summary of Results

In summary, this section has conducted two studies to understand 1) how the thickness of the thermochromic material affects the duration of the color-changing transition, and 2) how the temperature of Joule-heated conductive paths is distributed. The first experiment

reveals that 1 mm thickness is a suitable parameter for conveying the color-changing effect. The second experiment shows that the naïve approach of using resistive heating with simple infilled conductive cuboids is insufficient for activating the color-change transition on top of structures taller than 10 mm. For taller structures, in fact, the heat remains trapped close to the base, following the shortest path. These results provide a base understanding to further customize and integrate ThermoPixels into their 3D printed prototypes.

## 7 DISCUSSION AND LIMITATIONS

ThermoPixel's main contribution is to further expand on the idea of using selectively heated thermochromic flat displays [9, 45], and extend the potential of this technology to 3D geometries of arbitrary curved surfaces. As a result, ThermoPixels users are allowed to embed visual interfaces directly into 3D printed objects, without requiring manual and tedious fabrication processes used for currently existing spray-based displays. Instead, ThermoPixels rely on widely available conductive [34] and thermochromic [3] filaments for common FDM printers, and a 3D design tool that simplifies the design and placement of ThermoPixel primitives in existing geometries.

This work, however, also presents important limitations due to the ThermoPixels' power consumption, slow refresh rate, and their physical construction.

**Power Consumption.** A single ThermoPixel consumes about 1 W at 10-20 V per second when the heaters are active due to the large resistivity of the carbon-based conductive filament [34] (e.g., typical resistance of a pixel ranges between 100 and 500 Ohm). A possible workaround is to minimize the activation time of the thermochromic display, effectively lowering the dissipated power but also resulting in displays with slower color-changing transitions. Overall, we acknowledge the limitation of requiring high voltage, but we note that these values are nonetheless lower than those required by spray-painted EL displays [14], which typically work at 100V or 200V AC, and other conductive Joule-heating techniques [29, 49].

**Heat Bleed.** Our technical evaluation of ThermoPixels (referenced in section 3) demonstrates that their encapsulated design effectively reduces heat spread to adjacent areas. However, when ThermoPixels are left continuously active post color-change, heat gradually transfers to nearby parts of the geometry. Presently, our method involves manually managing the power supply, but future enhancements could include temperature monitoring using external tools (like thermal cameras or thermistors) or by integrating composite materials in the 3D printing process, such as copper filament [31], which could act as a resistance temperature detector.

**Slow Refresh time.** The slow refresh rate is due to the time necessary for Joule heating the thermochromic material. Assuming an ambient temperature of about 25 °C, our displays can currently draw an arbitrary image in about 11.75 seconds and need about 251 seconds for tuning off. This refresh rate is more than an order of magnitude slower than what possible with EL-based displays [14]. Although passive cooling lacks an external mechanism to expedite the process, resulting in a slower return to the original state, it allows ThermoPixels to remain 'ON' even without a continuous

power supply. This feature is particularly advantageous in certain applications where continuous power is not necessary, such as in a hand crank generator (as illustrated in Figure 16a). In these scenarios, the approach leverages the residual heat within the ThermoPixels, making passive cooling a beneficial compromise. A possible strategy to mitigate this problem could also be to use alternative sources of heat, such as laser beams [54] or Peltier modules [56]. Lasers have the advantage of requiring no contact with the color-changing surfaces but need a more complex setup and can only activate the part of the surface facing them. Peltiers have the advantage of providing both heating and cooling [56], but embedding these into arbitrary objects might be challenging.

Overall, we acknowledge this limitation, but we also believe that this hysteresis behavior is suitable for ambient displays that do not require fast activation. We also argue that ThermoPixels are not necessarily a competing alternative to other faster EL-based 3D displays [14, 33], but rather a complement. For example, we envision opportunities where fast-refreshing information could be provided on an EL layer, while long-lasting background information could be displayed with the thermochromic approach of the ThermoPixels. Finally, thermochromic displays offer a more durable and scratch-resistant solution for mechanical systems or parts (e.g., gears) when compared to EL displays, as these are very sensitive to impurities on their surface [14]. We think that future solutions will leverage both these two approaches.

**Construction.** Another limitation of the ThermoPixels is their minimum pixel size directly impacting the display resolution. ThermoPixels' size mainly depends on the conductive heater's size (footprint of 6 × 6 mm), which covers most part of the pixel's footprint. While increasing the size of the pixels with our current system is possible by integrating multiple heaters underneath a thermochromic surface, reducing the size of the pixel primitive remains challenging, as it requires 3D printing smaller heaters. In our empirical tests, we found that, due to the nozzle's size (0.4 mm), it is difficult to print, using an FDM printer, working heaters with a footprint smaller than 6 × 6 mm. One approach to address this issue is to fabricate a smaller thermochromic display atop a 6 × 6 mm heater footprint. The resolution of the thermochromic layer can be as fine as the printer nozzle's capability, which is 0.4 mm in this instance. We recognize this limitation of our system, but we also note that miniaturization is a common problem of functional prototypes printed with existing FDM machines.

Another limitation related to the construction of the ThermoPixels is that they require two different materials and a dual-nozzle printer. Although these kinds of printers are becoming more common and affordable, we recognize that many users might not have access to them. It is, however, possible to construct multi-filament surfaces using a single-nozzle printer [30, 35], but this approach typically requires a calibration process and manual swapping of filaments.

**Materials.** Finally, we recognize opportunities for using different types of off-the-shelf thermochromic filaments. We chose a material that activates at 32°C, but options for customization of the material are possible using different pigments [23]. The thermochromic filament can also be engineered with varying color transition temperatures, such as 40°C, 60°C [23], and 65°C [20], potentially enabling future displays to feature multiple color shifts

within the same pixel, triggered at these different temperatures. This versatility could also extend to applications in environments with higher ambient temperatures, such as extreme outdoor temperatures like 35°C and 40°C, where these varied thresholds would be particularly beneficial.

## 8 CONCLUSIONS

This paper contributes to the current effort within the HCI and digital fabrication community toward 3D printed interactive and functional prototypes [2, 7, 39] whose value is beyond the aesthetical and mechanical properties of an artifact. Specifically, this paper presents a method and a tool to construct a 3D display of arbitrary shapes using color-changing filament. This approach minimizes the need for post-printing manual fabrication and assembly of electronic components. These 3D printed displays are made of selectively controllable modules called ThermoPixels, which can be activated independently of each other and can be arranged to construct complex displays. We presented a design space for displays that are flat, textured, multi-color, curved, or flexible, and a set of applications that leverage these properties.

Future work will focus on expanding the vocabulary of these 3D displays using different methods for selective heating (e.g., lasers [54], Peltier modules [56]) or thermochromic filaments of other colors or with different activation temperatures [23]. Ultimately, we envision a future where printed prototypes will integrate sensing [39], actuating [2, 29], and, as shown in this paper, displaying capabilities in a single body and straight out of a 3D printer.

## ACKNOWLEDGMENTS

This work was supported by the National Research Foundation of Korea (NRF) grant funded by the Korea government (MSIT) (No. 2018R1A5A7025409).

## REFERENCES

- [1] AMOLEN. 2023. *Amolen 3D Filament Bundle*. [https://www.amazon.com/dp/B099JPZT2L?psc=1&ref=ppx\\_yo2ov\\_dt\\_b\\_product\\_details](https://www.amazon.com/dp/B099JPZT2L?psc=1&ref=ppx_yo2ov_dt_b_product_details)
- [2] Byoungkwon An, Ye Tao, Jianzhe Gu, Tingyu Cheng, Xiang 'Anthony' Chen, Xiaoxiao Zhang, Wei Zhao, Youngwook Do, Shigeo Takahashi, Hsiang-Yun Wu, Teng Zhang, and Lining Yao. 2018. *Thermorph: Democratizing 4D Printing of Self-Folding Materials and Interfaces*. Association for Computing Machinery, New York, NY, USA, 1–12. <https://doi.org/10.1145/3173574.3173834>
- [3] CC3D. 2023. *3D Printer Filament, heat-sensitive Thermochromic Filament Material*. [https://www.amazon.com/dp/B074T8TGL5?ref\\_=ast\\_sto\\_dp&th=1&psc=1](https://www.amazon.com/dp/B074T8TGL5?ref_=ast_sto_dp&th=1&psc=1)
- [4] COMSOL. 2017. *The Joule Heating Effect*. <https://www.comsol.com/multiphysics/the-joule-heating-effect>
- [5] Milena Djukanić, Ardijan Mavrić, Jovana Jovanović, Milovan Roganović, and Velibor Bošković. 2021. Design of 3D Printing Thermo-Sensored Medical Gear in Detecting COVID-19 Symptoms. *Applied Sciences* 11, 1 (2021). <https://doi.org/10.3390/app11010419>
- [6] Lifeng Dong, Steven Youkey, Jocelyn Bush, Jun Jiao, Valery M. Dubin, and Ramanan V. Chebiam. 2007. Effects of local Joule heating on the reduction of contact resistance between carbon nanotubes and metal electrodes. *Journal of Applied Physics* 101, 2 (2007), 024320. <https://doi.org/10.1063/1.2430769> arXiv:<https://doi.org/10.1063/1.2430769>
- [7] Charles El Helou, Philip R. Buskohl, Christopher E. Tabor, and Ryan L. Harne. 2021. Digital logic gates in soft, conductive mechanical metamaterials. *Nature Communications* 12, 1 (12 Mar 2021), 1633. <https://doi.org/10.1038/s41467-021-21920-y>
- [8] Ahmed Elkholly, Mahmoud Rouby, and Roger Kempers. 2019. Characterization of the anisotropic thermal conductivity of additively manufactured components by fused filament fabrication. *Progress in Additive Manufacturing* 4, 4 (01 Dec 2019), 497–515. <https://doi.org/10.1007/s40964-019-00098-2>
- [9] Shreyosi Endow, Mohammad Abu Nasir Rakib, Anvay Srivastava, Sara Rastegarpouryani, and Cesar Torres. 2022. Embr: A Creative Framework for Hand Embroidered Liquid Crystal Textile Displays. In *Proceedings of the 2022 CHI Conference on Human Factors in Computing Systems* (New Orleans, LA, USA) (CHI '22). Association for Computing Machinery, New York, NY, USA, Article 110, 14 pages. <https://doi.org/10.1145/3491102.3502117>
- [10] Patrick F. Flowers, Christopher Reyes, Shengrong Ye, Myung Jun Kim, and Benjamin J. Wiley. 2017. 3D printing electronic components and circuits with conductive thermoplastic filament. *Additive Manufacturing* 18 (2017), 156–163. <https://doi.org/10.1016/j.addma.2017.10.002>
- [11] Jun Gong, Olivia Seow, Cedric Honnet, Jack Forman, and Stefanie Mueller. 2021. *MetaSense: Integrating Sensing Capabilities into Mechanical Metamaterial*. Association for Computing Machinery, New York, NY, USA, 1063–1073. <https://doi.org/10.1145/3472749.3474806>
- [12] Daniel Groeger, Elena Chong Loo, and Jürgen Steimle. 2016. *HotFlex: Post-Print Customization of 3D Prints Using Embedded State Change*. Association for Computing Machinery, New York, NY, USA, 420–432. <https://doi.org/10.1145/2858036.2858191>
- [13] Ollie Hanton, Zichao Shen, Mike Fraser, and Anne Roudaut. 2022. FabricatINK: Personal Fabrication of Bespoke Displays Using Electronic Ink from Upcycled E Readers. In *Proceedings of the 2022 CHI Conference on Human Factors in Computing Systems* (New Orleans, LA, USA) (CHI '22). Association for Computing Machinery, New York, NY, USA, Article 173, 15 pages. <https://doi.org/10.1145/3491102.3501844>
- [14] Ollie Hanton, Michael Wessely, Stefanie Mueller, Mike Fraser, and Anne Roudaut. 2020. ProtoSpray: Combining 3D Printing and Spraying to Create Interactive Displays with Arbitrary Shapes. In *Proceedings of the 2020 CHI Conference on Human Factors in Computing Systems* (Honolulu, HI, USA) (CHI '20). Association for Computing Machinery, New York, NY, USA, 1–13. <https://doi.org/10.1145/3313831.3376543>
- [15] Chris Harrison and Scott E. Hudson. 2009. Texture Displays: A Passive Approach to Tactile Presentation. In *Proceedings of the SIGCHI Conference on Human Factors in Computing Systems* (Boston, MA, USA) (CHI '09). Association for Computing Machinery, New York, NY, USA, 2261–2264. <https://doi.org/10.1145/1518701.1519047>
- [16] Alexandra Ion, Johannes Frohnhofer, Ludwig Wall, Robert Kovacs, Mirela Alistar, Jack Lindsay, Pedro Lopes, Hsiang-Ting Chen, and Patrick Baudisch. 2016. Metamaterial Mechanisms. In *Proceedings of the 29th Annual Symposium on User Interface Software and Technology* (Tokyo, Japan) (UIST '16). Association for Computing Machinery, New York, NY, USA, 529–539. <https://doi.org/10.1145/2984511.2984540>
- [17] Walther Jensen, Ashley Colley, Jonna Häkkilä, Carlos Pinheiro, Markus Löchtefeld, and Marco Porta. 2019. TransPrint: A Method for Fabricating Flexible Transparent Free-Form Displays. *Adv. in Hum.-Comp. Int.* 2019 (jan 2019), 14. <https://doi.org/10.1155/2019/1340182>
- [18] Walther Jensen and Markus Löchtefeld. 2022. ECPlotter: A Toolkit for Rapid Prototyping of Electrochromic Displays. In *Proceedings of the 21st International Conference on Mobile and Ubiquitous Multimedia* (Lisbon, Portugal) (MUM '22). Association for Computing Machinery, New York, NY, USA, 1–11. <https://doi.org/10.1145/3568444.3568466>
- [19] Yuhua Jin, Isabel Qamar, Michael Wessely, Aradhana Adhikari, Katarina Bulovic, Parinya Punpongpanon, and Stefanie Mueller. 2019. Photo-Chromeleon: Re-Programmable Multi-Color Textures Using Photochromic Dyes. In *Proceedings of the 32nd Annual ACM Symposium on User Interface Software and Technology* (New Orleans, LA, USA) (UIST '19). Association for Computing Machinery, New York, NY, USA, 701–712. <https://doi.org/10.1145/3332165.3347905>
- [20] Yang Jin, Yanan Zhu, Xiaoqiang Li, and Mingqiao Ge. 2018. Thermosensitive luminous fibers based on cresol red-boric acid reversible thermochromic pigments. *Journal of Materials Science: Materials in Electronics* 29 (01 2018). <https://doi.org/10.1007/s10854-017-7897-z>
- [21] Jeeeon Kim and Tom Yeh. 2015. Toward 3D-Printed Movable Tactile Pictures for Children with Visual Impairments. In *Proceedings of the 33rd Annual ACM Conference on Human Factors in Computing Systems* (Seoul, Republic of Korea) (CHI '15). Association for Computing Machinery, New York, NY, USA, 2815–2824. <https://doi.org/10.1145/2702123.2702144>
- [22] Konstantin Klampka and Raimund Dachselt. 2017. IllumiPaper: Illuminated Interactive Paper. In *Proceedings of the 2017 CHI Conference on Human Factors in Computing Systems* (Denver, Colorado, USA) (CHI '17). Association for Computing Machinery, New York, NY, USA, 5605–5618. <https://doi.org/10.1145/3025453.3025525>
- [23] Donghyeon Ko, Yeeun Shin, Junbeom Shin, Jiwoo Hong, and Woohun Lee. 2022. ChromoFilament: Designing a Thermochromic Filament for Displaying Malleable States. In *Designing Interactive Systems Conference* (Virtual Event, Australia) (DIS '22). Association for Computing Machinery, New York, NY, USA, 1540–1554. <https://doi.org/10.1145/3532106.3533479>
- [24] Yong Lin Kong, Ian A. Tamargo, Hyoungsoo Kim, Blake N. Johnson, Maneesh K. Gupta, Tae-Wook Koh, Huai-An Chin, Daniel A. Steingart, Barry P. Rand, and Michael C. McAlpine. 2014. 3D Printed Quantum Dot Light-Emitting Diodes. *Nano Letters* 14, 12 (2014), 7017–7023. <https://doi.org/10.1021/nl5033292> PMID: 25360485. arXiv:<https://doi.org/10.1021/nl5033292> PMID: 25360485.

- [25] Liyu Liu, Suili Peng, Weijia Wen, and Ping Sheng. 2007. Paperlike thermochromic display. *Applied Physics Letters* 90, 21 (2007), 213508. <https://doi.org/10.1063/1.2742781> arXiv:<https://doi.org/10.1063/1.2742781>
- [26] Lumilor. 2023. *LUMILOR ELECTROLUMINESCENT COATING*. <https://www.lumilor.com/>
- [27] MAXIM. 2023. *MAXIM306CPI*. [https://www.mouser.kr/ProductDetail/Maxim-Integrated/MAX306CPI?qs=1THa7W0U59HP4j3BFfnzg\\$%3D%3D\\$](https://www.mouser.kr/ProductDetail/Maxim-Integrated/MAX306CPI?qs=1THa7W0U59HP4j3BFfnzg$%3D%3D$)
- [28] Alex Mazursky, Borui Li, Shan-Yuan Teng, Daria Shifrina, Joyce E Passananti, Svitlana Midianko, and Pedro Lopes. 2023. ThermalRouter: Enabling Users to Design Thermally-Sound Devices. In *Proceedings of the 36th Annual ACM Symposium on User Interface Software and Technology (<conf-loc>, <city>San Francisco</city>, <state>CA</state>, <country>USA</country>, </conf-loc>) (UIST '23)*. Association for Computing Machinery, New York, NY, USA, Article 58, 14 pages. <https://doi.org/10.1145/3586183.3606747>
- [29] Kongpyung (Justin) Moon, Haeul Lee, Jeeeon Kim, and Andrea Bianchi. 2022. ShrinkCells: Localized and Sequential Shape-Changing Actuation of 3D-Printed Objects via Selective Heating. In *Proceedings of the 35th Annual ACM Symposium on User Interface Software and Technology* (Bend, OR, USA) (UIST '22). Association for Computing Machinery, New York, NY, USA, Article 86, 12 pages. <https://doi.org/10.1145/3526113.3545670>
- [30] Mosaic. 2023. Palette 3Pro. <https://www.mosaicmfg.com/products/palette-3-pro>
- [31] Multi3D. 2022. *Electrifi Conductive Filament*. <https://www.multi3dllc.com/product/electrifi/>
- [32] Simon Olberding, Michael Wessely, and Jürgen Steinle. 2014. PrintScreen: Fabricating Highly Customizable Thin-Film Touch-Displays. In *Proceedings of the 27th Annual ACM Symposium on User Interface Software and Technology* (Honolulu, Hawaii, USA) (UIST '14). Association for Computing Machinery, New York, NY, USA, 281–290. <https://doi.org/10.1145/2642918.2647413>
- [33] Simon Olberding, Michael Wessely, and Jürgen Steinle. 2014. PrintScreen: Fabricating Highly Customizable Thin-Film Touch-Displays. In *Proceedings of the 27th Annual ACM Symposium on User Interface Software and Technology* (Honolulu, Hawaii, USA) (UIST '14). Association for Computing Machinery, New York, NY, USA, 281–290. <https://doi.org/10.1145/2642918.2647413>
- [34] Protopasta. 2022. *Protopasta Material Data*. <https://www.proto-pasta.com/pages/high-temp-pla#HTmade>
- [35] Josef Prusa. 2023. Original Prusa 3D printers directly from Josef Prusa. <https://www.prusa3d.com/>
- [36] Parinya Punpongsonan, Xin Wen, David S. Kim, and Stefanie Mueller. 2018. ColorMod: Recoloring 3D Printed Objects Using Photochromic Inks. In *Proceedings of the 2018 CHI Conference on Human Factors in Computing Systems* (Montreal QC, Canada) (CHI '18). Association for Computing Machinery, New York, NY, USA, 1–12. <https://doi.org/10.1145/3173574.3173787>
- [37] Fang Qin, Huai-Yu Cheng, Rachel Sneeringer, Maria Vlachostergiou, Sampada Acharya, Haolin Liu, Carmel Majidi, Mohammad Islam, and Lining Yao. 2021. ExoForm: Shape Memory and Self-Fusing Semi-Rigid Wearables. In *Extended Abstracts of the 2021 CHI Conference on Human Factors in Computing Systems* (Yokohama, Japan) (CHI EA '21). Association for Computing Machinery, New York, NY, USA, Article 249, 8 pages. <https://doi.org/10.1145/3411763.3451818>
- [38] SainSmart. 2023. *SainSmart Color-changing 95A TPU filament*. [https://www.amazon.com/dp/B0B9X94VN1?psc=1&ref=ppx\\_yo2ov\\_dt\\_b\\_product\\_details](https://www.amazon.com/dp/B0B9X94VN1?psc=1&ref=ppx_yo2ov_dt_b_product_details)
- [39] Martin Schmitz, Mohammadreza Khalilbeigi, Matthias Balwierz, Roman Lissermann, Max Mühlhäuser, and Jürgen Steinle. 2015. Capricate: A Fabrication Pipeline to Design and 3D Print Capacitive Touch Sensors for Interactive Objects. In *Proceedings of the 28th Annual ACM Symposium on User Interface Software and Technology* (Charlotte, NC, USA) (UIST '15). Association for Computing Machinery, New York, NY, USA, 253–258. <https://doi.org/10.1145/2807442.2807503>
- [40] Martin Schmitz, Jürgen Steinle, Jochen Huber, Niloofar Dezfouli, and Max Mühlhäuser. 2017. Flexibles: Formation-Aware 3D-Printed Tangibles for Capacitive Touchscreens. In *Proceedings of the 2017 CHI Conference on Human Factors in Computing Systems* (Denver, Colorado, USA) (CHI '17). Association for Computing Machinery, New York, NY, USA, 1001–1014. <https://doi.org/10.1145/3025453.3025663>
- [41] Ruitao Su, Sung Hyun Park, Xia Ouyang, Song Ih Ahn, and Michael C. McAlpine. 2022. 3D-printed flexible organic light-emitting diode displays. *Science Advances* 8, 1 (2022), eabl8798. <https://doi.org/10.1126/sciadv.abl8798> arXiv:<https://www.science.org/doi/pdf/10.1126/sciadv.abl8798>
- [42] Lingyun Sun, Yue Yang, Yu Chen, Jiaji Li, Danli Luo, Haolin Liu, Lining Yao, Ye Tao, and Guanyun Wang. 2021. ShrinCage: 4D Printing Accessories That Self-Adapt. In *Proceedings of the 2021 CHI Conference on Human Factors in Computing Systems* (Yokohama, Japan) (CHI '21). Association for Computing Machinery, New York, NY, USA, Article 433, 12 pages. <https://doi.org/10.1145/3411764.3445220>
- [43] David Sweeney, Nicholas Chen, Steve Hodges, and Tobias Grosse-Puppendahl. 2016. Displays as a Material: A Route to Making Displays More Pervasive. *IEEE Pervasive Computing* 15, 3 (2016), 77–82. <https://doi.org/10.1109/MPRV.2016.56>
- [44] Haruki Takahashi and Homei Miyashita. 2017. Expressive Fused Deposition Modeling by Controlling Extruder Height and Extrusion Amount. In *Proceedings of the 2017 CHI Conference on Human Factors in Computing Systems* (Denver, Colorado, USA) (CHI '17). Association for Computing Machinery, New York, NY, USA, 5065–5074. <https://doi.org/10.1145/3025453.3025933>
- [45] Cesar Torres, Jessica Chang, Advaita Patel, and Eric Paulos. 2019. Phosphenes: Crafting Resistive Heaters within Thermoreactive Composites. In *Proceedings of the 2019 on Designing Interactive Systems Conference* (San Diego, CA, USA) (DIS '19). Association for Computing Machinery, New York, NY, USA, 907–919. <https://doi.org/10.1145/3322276.3322375>
- [46] Arne Valberg, Bettina Lange-Malecki, and Thorstein Seim. 1991. Colour Changes as a Function of Luminance Contrast. *Perception* 20, 5 (1991), 655–668. <https://doi.org/10.1088/p200655> arXiv:<https://doi.org/10.1088/p200655> PMID: 1806907.
- [47] John Vlachopoulos and David Strutt. 2002. *Plastics Technician's Toolbox*. Vol. 2. Polydynamics, London.
- [48] Voxel8. 2023. *Voxel8*. <https://www.aniwaa.com/product/3d-printers/voxel8-3d-electronics-printer/>
- [49] Guanyun Wang, Tingyu Cheng, Youngwook Do, Humphrey Yang, Ye Tao, Jianzhe Gu, Byoungkwon An, and Lining Yao. 2018. *Printed Paper Actuator: A Low-Cost Reversible Actuation and Sensing Method for Shape Changing Interfaces*. Association for Computing Machinery, New York, NY, USA, 1–12. <https://doi.org/10.1145/3173574.3174143>
- [50] Guanyun Wang, Ye Tao, Ozguc Bertug Capunaman, Humphrey Yang, and Lining Yao. 2019. A-Line: 4D Printing Morphing Linear Composite Structures. In *Proceedings of the 2019 CHI Conference on Human Factors in Computing Systems* (Glasgow, Scotland UK) (CHI '19). Association for Computing Machinery, New York, NY, USA, 1–12. <https://doi.org/10.1145/3290605.3300656>
- [51] Guanyun Wang, Humphrey Yang, Zeyu Yan, Nurcan Gecer Ulu, Ye Tao, Jianzhe Gu, Levent Burak Kara, and Lining Yao. 2018. 4DMesh: 4D Printing Morphing Non-Developable Mesh Surfaces. In *Proceedings of the 31st Annual ACM Symposium on User Interface Software and Technology* (Berlin, Germany) (UIST '18). Association for Computing Machinery, New York, NY, USA, 623–635. <https://doi.org/10.1145/3242587.3242625>
- [52] Michael Wessely, Ticha Sethapakdi, Carlos Castillo, Jackson C. Snowden, Ollie Hanton, Isabel P. S. Qamar, Mike Fraser, Anne Roudaut, and Stefanie Mueller. 2020. Sprayable User Interfaces: Prototyping Large-Scale Interactive Surfaces with Sensors and Displays. In *Proceedings of the 2020 CHI Conference on Human Factors in Computing Systems* (Honolulu, HI, USA) (CHI '20). Association for Computing Machinery, New York, NY, USA, 1–12. <https://doi.org/10.1145/3313831.3376249>
- [53] Tonghao Wu, Tenghao Yin, Xiaocheng Hu, Guodong Nian, Shaoxing Qu, and Wei Yang. 2020. A Thermochromic Hydrogel for Camouflage and Soft Display. *Advanced Optical Materials* 8, 9 (2020), 2000031. <https://doi.org/10.1002/adom.202000031> arXiv:<https://onlinelibrary.wiley.com/doi/pdf/10.1002/adom.202000031>
- [54] Wenzheng Wu, Yiming Zhou, Qingping Liu, Luquan Ren, Fan Chen, Jerry Ying Hsi Fuh, Aodu Zheng, Xuechao Li, Ji Zhao, and Guiwei Li. 2023. Metallic 4D Printing of Laser Stimulation. *Advanced Science* 10, 12 (2023), 2206486. <https://doi.org/10.1002/advs.202206486> arXiv:<https://onlinelibrary.wiley.com/doi/pdf/10.1002/advs.202206486>
- [55] Tianyu Yu, Weiyi Xu, Haiqing Xu, Guanhong Liu, Chang Liu, Guanyun Wang, and Haipeng Mi. 2023. Thermotion: Design and Fabrication of Thermofluidic Composites for Animation Effects on Object Surfaces. In *Proceedings of the 2023 CHI Conference on Human Factors in Computing Systems* (Hamburg, Germany) (CHI '23). Association for Computing Machinery, New York, NY, USA, Article 425, 19 pages. <https://doi.org/10.1145/3544548.3580743>
- [56] Mason Zadan, Dinesh K. Patel, Andrew P. Sabelhaus, Jiae Liao, Anthony Wertz, Lining Yao, and Carmel Majidi. 2022. Liquid Crystal Elastomer with Integrated Soft Thermoelectrics for Shape Memory Actuation and Energy Harvesting. *Advanced Materials* 34, 23 (2022), 2200857. <https://doi.org/10.1002/adma.202200857> arXiv:<https://onlinelibrary.wiley.com/doi/pdf/10.1002/adma.202200857>